INTERNATIONAL JOURNAL OF INTEGRATED ENGINEERING
ISSN: 2229-838X e-ISSN: 2600-7916

IJIE

Vol. 16 No. 6 (2024) 182-195
https://publisher.uthm.edu.my/ojs/index.php/ijie

Impact of UHMWPE and PP Polymer Characterization on the Blending Process for PP/UHMWPE Composite in FFF

Fakrul Nur Aiman[1,2], Kamarudin.K[1,2]*, Rahim Jamian[1,2] , Shufeng Sun[3], M.F. Shaari[1,2], Mohd Nazrul Roslan[1,2], A. Ahmad[1,2], Mohd Khairuddin M.S[1], Raman.I[4]

[1] *Universiti Tun Hussein Onn Malaysia, 86400 Muar, Johor, MALAYSIA*
[2] *Innovative Manufacturing Technology (IMT) Focus Group, Universiti Tun Hussein Onn Malaysia, Hab Pendidikan Tinggi Pagoh, 84600 Muar, Johor, MALAYSIA*
[3] *School of Mechanical & Automotive Engineering, Qingdao University of Technology, Qingdao, 266520, CHINA*
[4] *Mechanical Engineering Department, Politeknik Merlimau, 77300 Merlimau, Melaka, MALAYSIA*

*Corresponding Author: khairu@uthm.edu.my
DOI: https://doi.org/10.30880/ijie.2024.16.06.018

Article Info

Received: 26 August 2024
Accepted: 11 October 2024
Available online: 4 November 2024

Keywords

Ultra-high molecular weight polyethylene, polypropylene, characterization, blending, composite

Abstract

Ultra-high molecular weight polyethylene (UHMWPE) is a thermoplastic semicrystalline polymer renowned for its exceptional wear resistance, low friction coefficient, and robust mechanical properties. It also exhibits strong resistance to corrosive substances. Despite these unique characteristics, UHMWPE has an extremely low melt flow rate (MFR) near zero, making it unsuitable for traditional polymer processing techniques. To address this issue, polypropylene (PP) is often used as a plasticizer to enhance the extrudability of UHMWPE-based composites. PP, a widely used thermoplastic polymer, is synthesized from the monomer propylene via chain-growth polymerization. However, chemical incompatibility between UHMWPE and PP poses challenges in composite manufacturing. This research aims to examine the characteristics of both materials to better understand the requirements and impact of these properties on the blending process of UHMWPE-PP composites for Fused Filament Fabrication (FFF). The characterization process includes analyzing the morphological, thermal behaviour and stability, and crystallinity of UHMWPE and PP in their respective powder and granular forms. The study reveals how the particle shape influences the behaviour of both polymers and the outcomes of their blending. Comprehensive characterization informs the blending process, ensuring a homogeneous mixture and improved interfacial adhesion. The discoveries presented in this paper are implemented in examining the extrudability of UHMWPE-PP composites, incorporating various blending materials, for the specific application of bone repair implants using FFF.

1. Introduction

Ultra-high molecular weight polyethylene (UHMWPE) boasts distinctive properties, including non-toxicity, simple chemical composition and structure, low water absorption, and resistance to chemicals and radiation [1-2]. Due to its high molecular weight, UHMWPE has an extremely low melt flow rate (MFR) of approximately zero, making it unsuitable for standard polymer processing methods [3-6]. Recently, various materials have been combined with plasticizing agents like polypropylene (PP) [7], polyethylene glycol (PEG) [8], high-pressure polyethylene (HDPE), alpha-tocopherol (vitamin E), and hydroxyapatite (HA) to enhance the viscosity of UHMWPE [9-10].

However, recent studies indicate that plasticizers partially degrade the structure of UHMWPE. They also reduce the mechanical and tribological properties of two- or three-component UHMWPE-based composites. Polypropylene (PP) is a thermoplastic polymer widely used across many industry sectors [11-13]. Made from the monomer propylene using chain-growth polymerization, PP has high heat resistance, allowing products to be aseptic at temperatures up to 145°C [14-15]. Additionally, PP is characterized by a high MFR of about 0.5-2.0 g/10 min [16-18]. These properties make PP one of the most promising plasticizers for enhancing the extrudability of UHMWPE-based composites [19-20]. Utilizing PP-UHMWPE composites addresses two issues: enhancing the wear resistance of the polymer and enabling the production of complexly shaped products through Fused Filament Fabrication (FFF) using 3D printing techniques [21-22]. Manual shaking or hand mixing has been found ineffective in achieving homogeneous integration of different polymer forms, such as powder and granular [23-26]. As a result, homogeneous blends are formed using melt blending in line with the specified weight percentages [27].

Blending PP with UHMWPE aims to combine their advantageous properties. PP improves the extrudability of UHMWPE, known for its wear resistance and low friction but challenging melt flow rate [28]. Characterizing thermal, mechanical, and rheological properties is crucial in the blending process to ensure compatibility and uniformity [29-30]. Effective blending addresses inherent compatibility issues, yielding composites suitable for FFF with potential applications like bone repair implants [31-33]. This study aims to analyse the properties of both polymers to improve blending and FFF extrudability. It seeks to foster a deeper understanding and increase the likelihood of successful composite production. Additionally, the outcomes of successful composite production will be examined to determine the optimal composite material blending.

2. Methodology

A comprehensive approach is taken to study the properties of raw polypropylene (PP) and ultra-high-molecular-weight polyethylene (UHMWPE). The study details the materials used and the analytical methods applied. It provides insights into the particle size, morphology, and structural characteristics of these polymers using advanced techniques. Mixing parameters like speed, time, and temperature are carefully controlled to prevent degradation and ensure consistency. The mixture is periodically sampled and inspected microscopically to verify uniform particle distribution. This thorough examination highlights the inherent properties of PP and UHMWPE and emphasizes the importance of controlled mixing for reliable and reproducible results.

2.1 Materials

The polypropylene (PP) utilized in this research meets medical grade standards and is supplied in granular form by Emory. Conversely, the ultra-high molecular weight polyethylene (UHMWPE) utilized is Medical Grade GUR1020 intended for surgical implants and was provided by Emory in powdered form [9], [34]. Both materials are distinguished by their specs, as indicated in Table 1. Table 2 illustrates the blend compositions and material designations utilized in this study. Additionally, an additional composition, specifically 5%, along with a 10% increase in the additive proportion, was included for further investigation within the critical range.

2.2 Method

This study uses various analytical techniques to thoroughly examine and characterize Polypropylene (PP) and Ultra-High Molecular Weight Polyethylene (UHMWPE) polymers, including their mixing process.

2.2.1 Scanning Electron Microscope (SEM)

A scanning electron microscope (SEM) is a high-resolution imaging tool used in various scientific fields. It works by directing electrons onto a sample and capturing emitted signals like secondary electrons, backscattered electrons, and characteristic X-rays [35]. SEMs create detailed images of a sample's surface morphology and composition, which is useful in materials science, biology, geology, and nanotechnology [36].

In this study, the surface morphology of the samples was examined using a COXEM EM-30AX SEM after a 24-hour drying process. Samples were mounted on carbon tapes attached to upright stubs and pre-coated with gold to reduce charge reflection. Observations were made under vacuum conditions at 1.0k magnification and 20.0 kV

accelerating voltage. The magnification ranged from 200x to 2.0k to analyze particle size, shape, and potential contamination

Table 1 *Specification of polymer material*

Specification	Polypropylene (PP)	UHMWPE
Density (g/cm^3)	0.9	0.93
Molecular Weight (g/mol)	620,000	5,000,000
Yield Tensile Strength (MPa)	27.5	21
Flexural Modulus (MPa)	1320	-
Notched Izd Impact (kJ/m^2)	-	210

Table 2 *Sample designation for both materials*

Designation	PP (wt%)	UHMWPE (wt%)
PP + UHMWPE – 5%	95	5
PP + UHMWPE – 10%	90	10
PP + UHMWPE – 20%	80	20
PP + UHMWPE – 30%	70	30
PP + UHMWPE – 40%	60	40
PP + UHMWPE – 50%	50	50

2.2.2 X-Ray Diffraction (XRD)

A fully crystalline material shows sharp peaks in its XRD pattern, indicating reflections from specific crystallographic planes. In contrast, an amorphous material displays a broad peak, representing the average distance between polymer chains. Semi-crystalline polymers show a mix of sharp crystalline reflections and a broad amorphous halo in their XRD patterns. Crystallinity can be measured by comparing the intensity of crystalline peaks to the total XRD curve area [37-38].

For the analysis, granular PP was crushed into powder and dried for 24 hours. The samples were mounted on plates and inserted into a Bruker D2 PHASER 2nd generation XRD machine. They were scanned from 10° to 70° with a step size of 0.05° and a time per step of 10 seconds, using Cu Kα radiation (λ = 1.5406 Å) within a 2θ range of 10-80° and a step size of 0.01°. The data was processed with Origin software, identifying crystalline phases by matching XRD peaks with standard PDF files using Eva Diffrac Plus (Version 4) [37-38].

2.2.3 Fourier Transform Infrared (FTIR)

FTIR spectroscopy, using Fourier transform technology, is a widely used analytical method for studying polymeric materials. It's been extensively employed for over two decades to scrutinize microscopic regions within polymers, aided by integrating an infrared interferometer with a microscope and specialized detectors. Recent advancements in instrumentation, like focal plane array (FPA) detectors, have further broadened the scope of FTIR spectroscopy applications [39-41].

Recent advancements in FTIR micro spectroscopy have significantly improved its instrumental capabilities and visualization techniques, particularly for studying multicomponent polymer systems. Utilizing FTIR (Perkin Elmer Spectrum One) with a universal diamond attenuated total reflection (ATR), functional groups of both materials were identified across a wavenumber range of 400 cm^{-1} to 4000 cm^{-1}. Powdered UHMWPE and small PP granules were placed in the testing area, aiming to gather information on the polymers' bonding, chemical class, and molecular structure.

2.2.4 Degree of Crystallinity

The crystallinity of polymers significantly affects their chemical and mechanical properties, such as Young's modulus, yield stress, strength, fatigue resistance, and shrinkage. The degree of crystallinity in polymers can be measured using various techniques, including thermal analysis, volumetric analysis, infrared spectroscopy, Raman spectroscopy, and X-ray diffraction. Each of these methods provides different results because they assess distinct physical characteristics and morphological features of the polymers [42]. XRD techniques were applied in this investigation to measure the degree of crystallinity of both UHMWPE and PP based on their own form approach.

X-ray diffraction is a commonly used method for evaluating the crystallinity level in polymers. In this technique, sharp peaks in the diffraction profile signify the presence of crystallites, while broad peaks represent the scattering from the amorphous phase. The intensity of this scattering can be measured and quantified to determine the degree of crystallinity using a specific equation (1) below [43]:

$$X_C(\%) = \frac{I_C}{I_C + I_A} \times 100 \quad (1)$$

IC and IA are the scattered intensities for the crystalline and the amorphous phases, respectively. The degree of crystallinity was calculated using Equation (2) [43-44]. The theory posits that the areas under the peaks are proportional to the scattering intensities of both the crystalline and amorphous phases. AC represents the area of crystalline phase (i.e., A110 +A200) and AA is the area of amorphous phase.

$$X_C(\%) = \frac{A_C}{A_C + A_A} \times 100 \quad (2)$$

2.2.5 Material Blending

The desired blend ratio of PP and UHMWPE was determined by 40g weight, and the appropriate quantities ratio of each polymer was weighed accordingly. The Brabender Plastograph EC plus as per Figure 1 that being used was preheated to a temperature of 170℃ above the melting points of both polymers to ensure proper melting and mixing. Once the plastograph reached the target temperature, the PP granule and UHMWPE powdered were introduced into the close mixing chamber, and the twin-screw mechanism was activated to generate intense shear forces for thorough intermixing [45-46].

The mixing process was maintained for 10-20 minutes duration, with continuous monitoring of torque and temperature to ensure consistent processing conditions. After the mixing cycle, the blended material was carefully extracted from the plastograph and allowed to cool and solidify. The resulting composite material was analysed to assess the homogeneity and distribution of the polymer components, ensuring that the blending process using the Brabender Plastograph with a twin-screw mechanism and close mixing chamber resulted in an efficient and uniform mixture of PP and UHMWPE.

Fig. 1 *Brabender Plastograph EC Plus*

3. Result and Discussion

The analysis of PP and UHMWPE provides valuable insights into their fundamental properties. By integrating data from a variety of analytical techniques, this study enhances the understanding of the characteristics of both PP and UHMWPE, thereby facilitating their effective use in combination. The results and discussion presented herein elucidate the distinctive differences and similarities between these two polymers, highlighting their respective advantages and limitations. Additionally, the mixing process and its results are thoroughly examined, revealing

Int. Journal of Integrated Engineering Vol. 16 No. 6 (2024) p. 182-195

how parameters such as speed, time, and temperature influence the uniformity and stability of the blend. This comprehensive analysis underscores the importance of controlled mixing in optimizing the performance and application of these polymers.

3.1 X-Ray Diffraction (XRD)

Fig. 2(a) presents the X-ray diffraction (XRD) spectrum of UHMWPE powder, revealing its semi-crystalline nature. The spectrum displays distinct peaks at 22.5° (110) and 24° (200), characteristic of the orthorhombic crystalline phase typical of polyethylene. These peaks indicate the presence of well-ordered crystalline regions within the polymer, with the remaining amorphous phase contributing to the overall semi-crystalline structure. The clarity and intensity of these peaks suggest a relatively high degree of crystallinity, which can impact the polymer's mechanical and thermal properties.

In Fig. 2(b), the XRD spectrum of granular polypropylene (PP) is shown, also confirming its semi-crystalline nature. The spectrum features sharp diffraction peaks at approximately 14° and 17°, indicative of polypropylene's orthorhombic crystal structure. The intensity and sharpness of these peaks reflect well-defined crystalline regions within the polymer chain, signifying a significant level of order and regularity in the PP sample. This ordered structure contributes to the material's strength and stability [47-48].

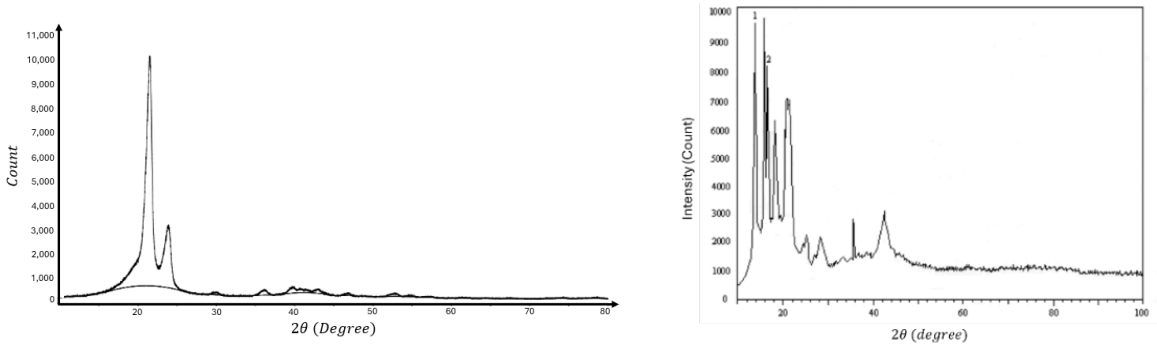

(a) **(b)**

Fig. 2 *XRD (a) Raw UHMWPE; (b) Raw PP*

These findings highlight the crystalline characteristics of both UHMWPE and PP, providing insights into their structural properties. The distinct and sharp peaks observed in the XRD spectra align with those reported in existing research [47-48], confirming the presence of crystalline phases and enhancing the understanding of the polymers' structural attributes. This analysis underscores the importance of crystallinity in influencing the physical properties of the materials, such as their mechanical strength and thermal resistance.

3.2 Fourier Transform Infrared (FTIR)

Fig. 3 presents the Fourier-transform infrared (FTIR) spectrum of UHMWPE, which reveals several key absorption features. Prominent absorption bands at 2917 cm^{-1} and 2844 cm^{-1} correspond to methylene stretching, while peaks at 1461 cm^{-1} and 1357 cm^{-1} are attributed to methyl bending. Additionally, weak bands at 716 cm^{-1} indicate C-H wagging. These features are characteristic of aliphatic chains and saturated hydrocarbons. The lack of absorption peaks in the 2140-2085 cm^{-1} (carbonyl) and 3600-3200 cm^{-1} (hydroxyl) regions suggests minimal functionalization of the UHMWPE. Overall, this analysis confirms that UHMWPE is primarily composed of hydrocarbon molecules with aliphatic chains.

Fig. 4 shows the FTIR spectrum of raw polypropylene (PP), highlighting distinct absorption bands in the 2800-3000 cm^{-1} range, indicative of aliphatic methyl (-CH_3) and methylene (-CH_2-) groups. A strong peak at 2970 cm^{-1} corresponds to symmetric CH_2 stretching, while a peak at 2845 cm^{-1} indicates asymmetric CH_3 stretching [49]. In the C-H bending region (1460-1375 cm^{-1}), observable peaks correspond to the bending vibrations of methyl and methylene groups. Specifically, the peak at approximately 1454 cm^{-1} is associated with symmetric bending of CH_3 groups, while the peak near 1372 cm^{-1} is linked to asymmetric bending of CH_3 groups.

These FTIR analyses provide valuable insights into the chemical composition and molecular arrangement of UHMWPE and PP. The results are consistent with known spectral features for these polymers, confirming their hydrocarbon-based structure and aiding in the understanding of their chemical properties and potential applications.

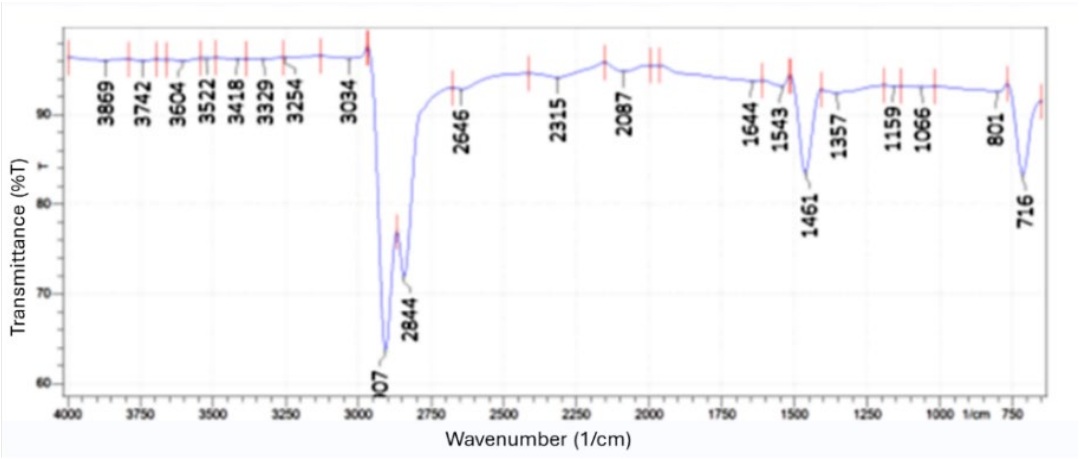

Fig. 3 *FTIR on virgin UHMWPE powder*

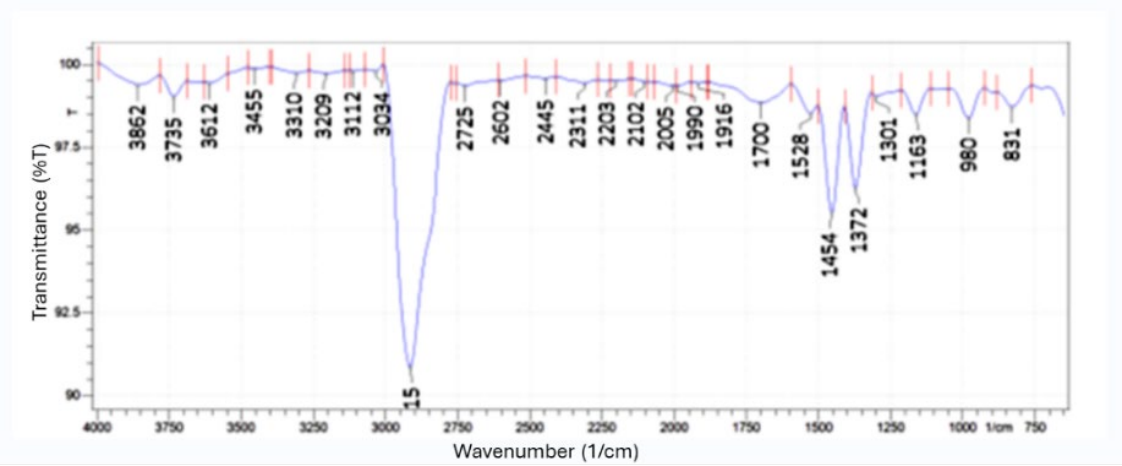

Fig. 4 *FTIR on virgin PP granules*

3.3 Scanning Electron Microscope (SEM)

UHMWPE particles, approximately 10 µm in size and elongated, exhibit exceptional toughness and wear resistance. In contrast, PP particles range from micrometer to sub-micrometer sizes and have finer grain structures that confer flexibility. This implies that PP, with its larger average particle size, serves as the primary matrix material, while UHMWPE acts as a filler to enhance the composite's properties. Scanning Electron Microscopy (SEM) analysis of UHMWPE particles, as shown in Figure 5, reveals their highly agglomerated, non-spherical, and porous nature [3].

At 200x magnification (Fig. 5(a)), UHMWPE powder particles appear generally uniform in shape with some variation in size and morphology, though fibrils are not distinctly visible. At 500x magnification (Fig. 5(b)), individual particle shapes and elongated, thread-like fibrils within the UHMWPE matrix become more apparent. Further, at 1000x magnification (Fig. 5(c)), the morphology of particles and fibril networks is pronounced, showing more detailed structural features. At 2000x magnification (Fig. 5(d)), nanoscale features and the alignment of fibrils are clearly observable, providing detailed insights into the material's structure. The irregular surface structure of UHMWPE reduces its ability to pack into regular formations.

In contrast, Figure 6 shows the SEM images of PP granules. At 500x magnification (Fig. 6(a)), the PP surface appears smooth and featureless. As magnification increases to 1000x (Fig. 6(b)), moderate roughness becomes visible, with sporadic shallow depressions and small protuberances, likely resulting from the manufacturing process and cooling history. At 2000x magnification (Fig. 6(c)), distinct crystalline regions with a granular texture, interspersed within an amorphous matrix, are evident, indicating non-uniform nucleation and growth during polymer solidification.

3.4 Degree of Crystallinity

XRD analysis was utilized to evaluate the degree of crystallinity for both UHMWPE powder and PP granules, with the findings presented in Table 3.

Int. Journal of Integrated Engineering Vol. 16 No. 6 (2024) p. 182-195

Table 3 *Degree of crystallinity (Xc) of UHMWPE and PP*

Material	Crystallinity (%)
UHMWPE Powder	63.63 ± 0.50
PP Granular	71.43 ± 0.50

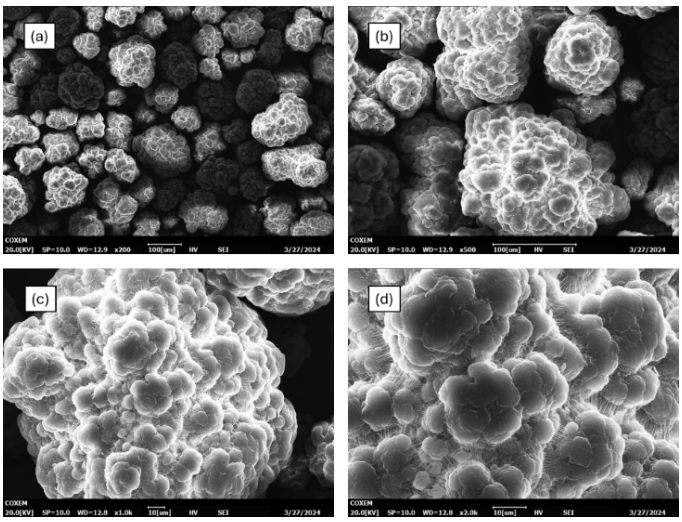

Fig. 5 *Scanning electron microscopy (SEM) images of virgin UHMWPE powder. The image shows the irregular structure and non-spherical shape. Magnifications: (a) 200×; (b) 500×; (c) 1000× and (d) 2000×*

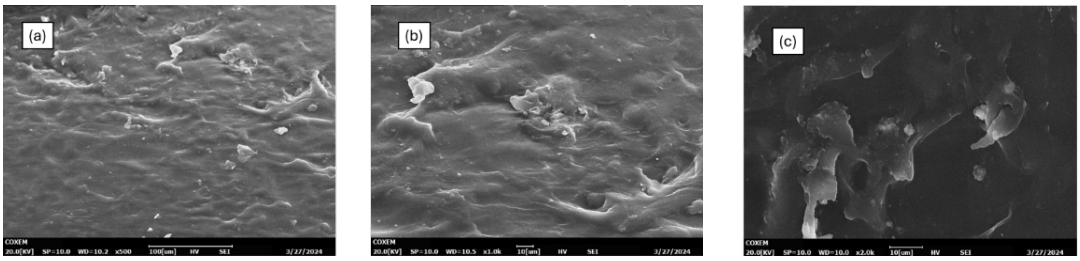

Fig. 6 *Scanning electron microscopy (SEM) images of virgin PP granular form. The image shows smooth and featureless. Magnifications: (a) 500×; (b) 1000×; and (c) 2000×*

According to Dong (2021), the crystallinity (Xc) of UHMWPE can range broadly from 29% to 65% [50]. XRD analysis is instrumental in providing insights into the crystalline structure of these materials. For UHMWPE, distinct peaks at 22.5° and 24° correspond to the (110) and (200) crystallographic planes, indicative of ordered crystalline regions within the material. The crystallinity percentage was calculated by integrating the intensity of these peaks, accounting for the background or amorphous contribution. The degree of crystallinity for UHMWPE, as calculated using the formula:

$$X_C(\%) = \frac{700}{700 + 400} \times 100 \tag{3}$$

$$X_C(\%) = 63.63\% \tag{4}$$

This value indicates that approximately 63.63% of UHMWPE's composition consists of ordered crystalline regions, reflecting its structural integrity and providing a basis for further characterization. Similarly, for PP granules, XRD peaks at 14° and 17° were analyzed. The crystallinity was determined using a similar approach, resulting in:

$$X_C(\%) = \frac{1000}{1000 + 400} \times 100 \tag{5}$$

$$X_C(\%) = 71.43\% \tag{6}$$

The higher crystallinity of PP, approximately 71.43%, suggests a greater proportion of crystalline regions compared to UHMWPE. This reflects better organization of polymer chains into crystalline structures, which typically enhances mechanical properties such as stiffness and strength. However, the degree of crystallinity can be influenced by processing conditions, molecular weight, and additives. Hence, precise characterization techniques like XRD are crucial for a comprehensive understanding of material properties and their implications for performance.

3.5 Blending of PP/UHMWPE

In this study, the successful blending of PP and UHMWPE was achieved using a Brabender internal mixer. The analysis focuses on various aspects of the blending process, including control parameters and efficiency improvements. Detailed data on these factors have been discussed and examined to ensure optimal blending performance. The findings are critical for understanding the percentage of blending achieved and ensuring homogeneity in the final composite.

3.5.1 Homogenous Mixing

Fig. 7 and 8 depict the torque and temperature profiles for PP/UHMWPE blends with varying UHMWPE content. Fig.e 7(a) illustrates the 95% PP / 5% UHMWPE blend, where the initial torque peak is modest, and the torque quickly stabilizes at a lower level. The minimal UHMWPE content results in a relatively smooth blending process with limited viscosity fluctuations. The temperature profile shows a typical rise as PP melts and integrates with the small amount of UHMWPE.

In Figure 7(b), the 90% PP / 10% UHMWPE blend exhibits a slightly higher initial torque peak compared to the 95% PP / 5% UHMWPE blend, reflecting the increased UHMWPE presence. The torque stabilizes relatively quickly, indicating good miscibility and moderate viscosity increases. The temperature profile remains stable with no significant fluctuations. Fig. 7(c) shows the 80% PP / 20% UHMWPE blend, where the initial torque peak is more pronounced and the stabilization period is longer. This indicates a greater impact of UHMWPE on the blend's viscosity, with a higher torque plateau signifying increased resistance during mixing. The temperature profile suggests a longer time to achieve homogeneity but eventually stabilizes

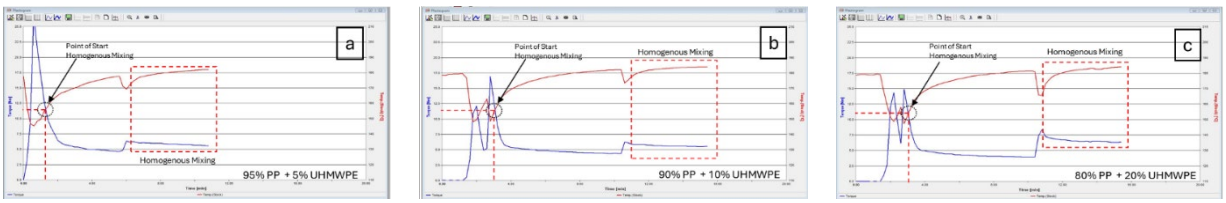

(a) **(b)** **(c)**

Fig. 7 *Graph of Torque vs Temperature: (a) 95% PP + 5% UHMWPE; (b) 90% PP + 10% UHMWPE; (c) 80% PP + 20% UHMWPE*

Fig. 8(a) through 8(c) further illustrates the effects of higher UHMWPE content. In Fig. 8(a), the 70% PP /30% UHMWPE blend shows a notable increase in the initial torque peak and a prolonged stabilization phase, with more fluctuations in the torque curve before reaching stability. The temperature profile indicates a more challenging mixing process, requiring more effort to achieve uniformity.

Figure 8(b) depicts the 60% PP / 40% UHMWPE blend, where the initial torque peak is substantial, and the stabilization phase is extended. The increased UHMWPE content results in a higher and more unstable torque plateau, with noticeable fluctuations in the temperature profile and significant effort needed for consistent mixing. Figure 8(c) shows the 50% PP / 50% UHMWPE blend, which has the highest initial torque peak and the longest stabilization phase. The equal proportions of PP and UHMWPE present substantial mixing challenges due to high viscosity and differing polymer properties, with pronounced torque fluctuations before stabilization and considerable energy input required for achieving a uniform blend.

Int. Journal of Integrated Engineering Vol. 16 No. 6 (2024) p. 182-195

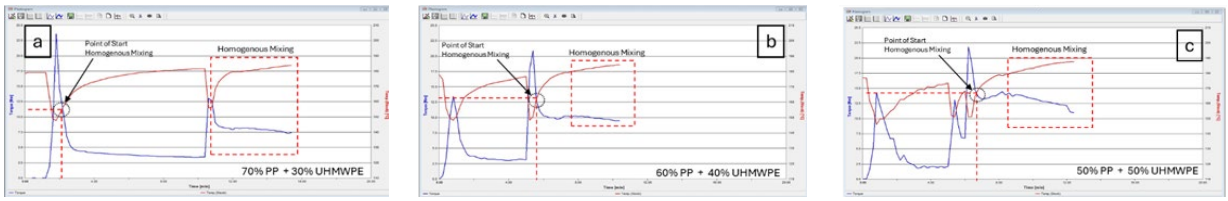

(a) **(b)** **(c)**

Fig. 8 *Graph of Torque vs Temperature; (a) 70% PP + 30% UHMWPE; (b) 60% PP + 40% UHMWPE; (c) 50% PP + 50% UHMWPE*

Overall, as UHMWPE content increases, the initial torque peak and the time required to reach a stable torque plateau rise, reflecting higher viscosity and greater mixing challenges. The blends with lower UHMWPE content (95% PP / 5% UHMWPE and 90% PP / 10% UHMWPE) demonstrate relatively smooth and quick stabilization. In contrast, blends with higher UHMWPE content (80% PP / 20% UHMWPE and above) require more effort and time to achieve homogeneity, with significant mixing challenges observed in the 60% PP / 40% UHMWPE and 50% PP / 50% UHMWPE blends. These findings underscore the critical role of UHMWPE content in influencing the processing behavior and compatibility of PP/UHMWPE blends.

3.5.2 Difference Weight of Ratio PP/UHMWPE Composite

Figure 9 illustrates the relationship between the weight and weight difference of PP/UHMWPE composites at various ratios. The x-axis represents the different PP to UHMWPE ratios, ranging from the container alone to blends of 95% PP / 5% UHMWPE, 90% PP / 10% UHMWPE, 80% PP / 20% UHMWPE, 70% PP / 30% UHMWPE, 60% PP / 40% UHMWPE, and 50% PP / 50% UHMWPE. The y-axis measures the weight in grams. Initially, the container weight is 14.06 grams. As UHMWPE content increases, the composite weight rises significantly, from 47.46 grams at the 95% PP / 5% UHMWPE ratio to 53.52 grams at the 50% PP / 50% UHMWPE ratio, indicating a positive correlation between UHMWPE proportion and overall composite weight.

The graph also presents the weight difference for each ratio, which increases in tandem with UHMWPE content. For the 95% PP / 5% UHMWPE blend, the weight difference is 33.40 grams, rising to 39.46 grams for the 50% PP / 50% UHMWPE blend. This consistent increase underscores the impact of UHMWPE on the composite's weight characteristics. The dotted lines on the graph illustrate a linear trend, confirming that both the total weight and weight difference increase steadily with higher UHMWPE content. Overall, the graph effectively demonstrates that higher UHMWPE proportions in the PP matrix result in heavier composites, with both weight and weight difference metrics showing a clear linear progression, highlighting UHMWPE's significant role in determining the composite's weight properties.

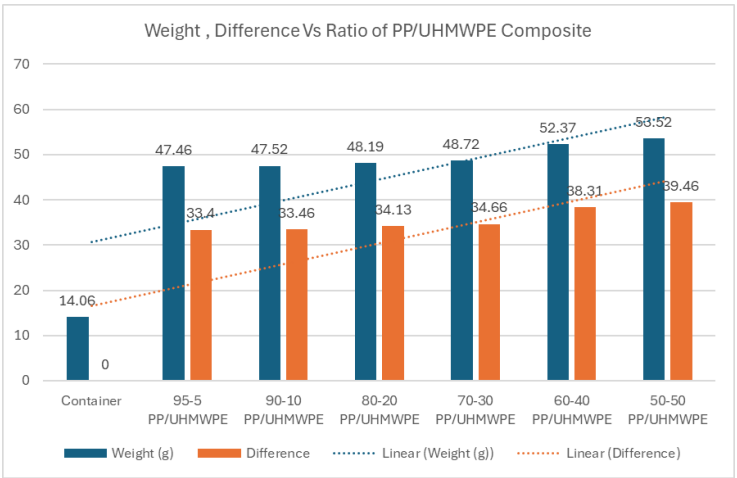

Fig. 9 *Graph of weight and difference based on ratio of composite*

3.5.3 Percentage Loss of PP/UHMWPE Composite with Actual Weight

Fig. 10 depicts the actual weight, original weight, and percentage loss of PP/UHMWPE composites at different ratios, ranging from 95% PP / 5% UHMWPE to 50% PP / 50% UHMWPE. The blue line represents the original

weight, which remains constant at approximately 40 grams across all ratios, reflecting the expected weight before processing. The orange bars show the actual weight of the composites, which decreases from around 33 grams at the 95% PP / 5% UHMWPE ratio to about 37 grams at the 50% PP / 50% UHMWPE ratio. The green line indicates the percentage loss, which decreases significantly from approximately 15% at the 95% PP / 5% UHMWPE ratio to about 2% at the 50% PP / 50% UHMWPE ratio. This trend implies that as the UHMWPE content increases, the actual weight of the composites approaches the original weight, suggesting reduced material loss during processing. Higher UHMWPE content appears to enhance thermal stability or reduce degradation rates of the composites, leading to better material retention. Therefore, increasing UHMWPE in the composite results in lower weight loss, which is advantageous for applications where maintaining the composite's weight is crucial.

Fig. 11 illustrates the percentage loss of actual weight for PP/UHMWPE composites across six trials, with the x-axis representing the trial number and the y-axis showing the percentage loss, ranging from 0% to 25%. The graph reveals a clear downward trend, with a linear trend line described by the equation:

$$y = -0.0324x + 0.2242 \tag{7}$$

This equation indicates a linear decrease in weight loss over the trials. Initially, the weight loss is 17% in the first trial and decreases to 16% in the second trial. By the third trial, the loss reduces to 15%, and continues to decline to 13% by the fourth trial. A notable reduction is observed in the fifth trial, where weight loss drops to 4%, and by the sixth trial, it is minimal at 1%. This trend suggests that the composite's stability improves over successive trials, with a reduction in weight loss indicating enhanced material performance and resistance to degradation. The linear equation can assist in optimizing weight combinations for desired blending compositions while ensuring effective weight retention.

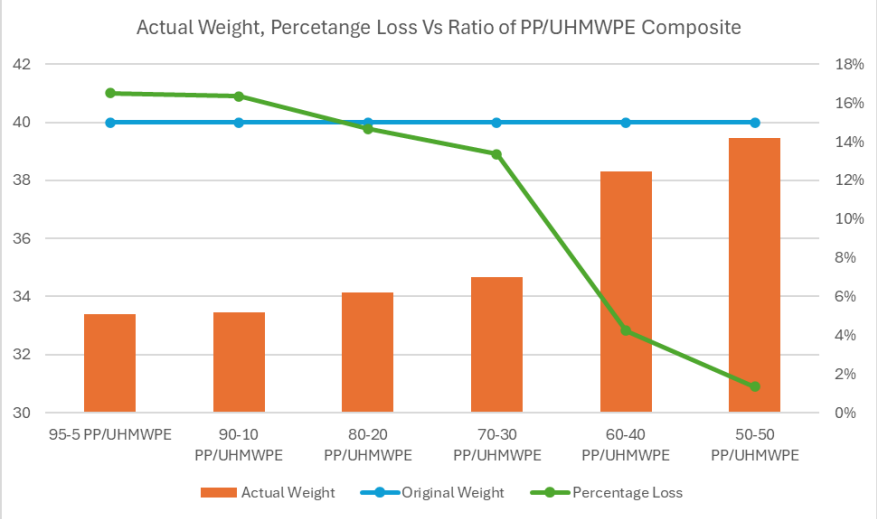

Fig. 10 *Graph of actual weight and percentage loss based on ratio of composite*

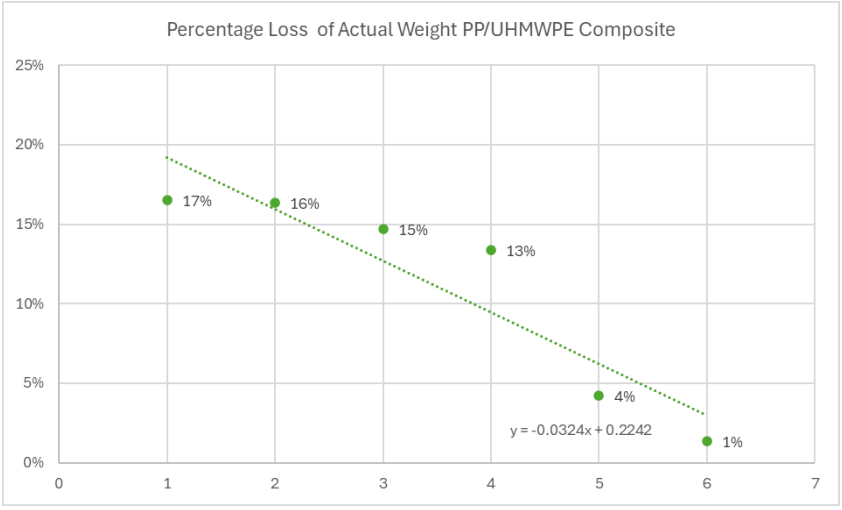

Fig. 11 *Scatter graph of percentage loss with equation analysis*

Int. Journal of Integrated Engineering Vol. 16 No. 6 (2024) p. 182-195

3.5.4 Time Taken to Achieve Homogenous Mixing

Graph in Fig. 12 provides an analysis of the mixing times for PP/UHMWPE composites at various ratios. The x-axis shows the PP to UHMWPE ratios, ranging from 95% PP / 5% UHMWPE to 50% PP / 50% UHMWPE, while the y-axis on the left indicates the time required to start and achieve homogeneous mixing in minutes. The y-axis on the right represents the total mixing time. The orange bars illustrate that initiation time increases from approximately 1.5 minutes for the 95% PP / 5% UHMWPE ratio to about 3.5 minutes for the 50% PP / 50% UHMWPE ratio, showing that higher UHMWPE content extends the time needed to begin mixing.

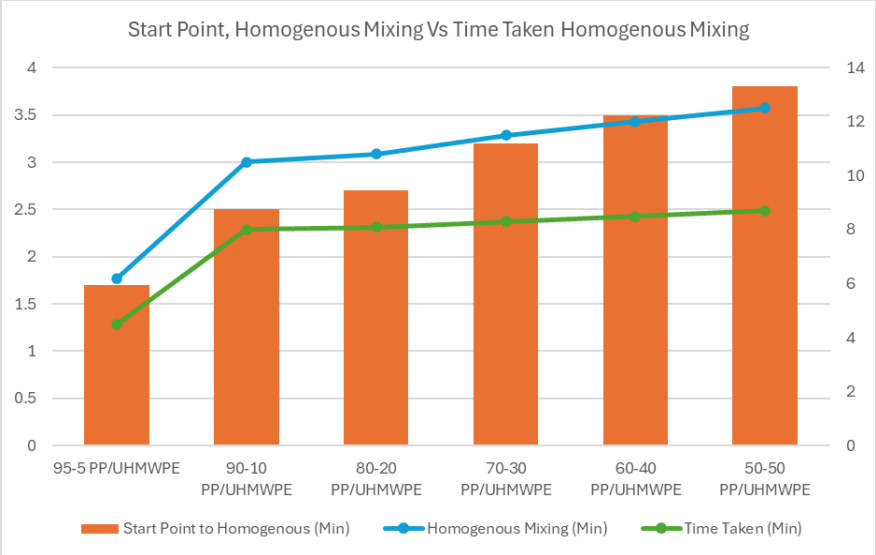

Fig. 12 *Graph of starting point, homogenous mixing with time taken*

The blue line represents the total time required to achieve a homogeneous mix, which increases from around 2.5 minutes for the 95% PP / 5% UHMWPE ratio to approximately 3.5 minutes for the 50% PP / 50% UHMWPE ratio. This indicates that more UHMWPE requires a longer time to reach uniformity. Conversely, the green line shows that the time required to maintain a homogeneous mixture remains constant at about 11 minutes across all ratios, suggesting that once a uniform mixture is achieved, its stability is unaffected by UHMWPE content. These results suggest that while higher UHMWPE content complicates the initial mixing process and extends the total mixing time, it does not impact the time needed to maintain a homogeneous mixture. This is consistent with existing research, which indicates that increased filler content can affect initial processing but not the final mixture's stability. For practical applications, this means that although initial processing may be more challenging with higher UHMWPE ratios, the final product remains stable, and manufacturers can plan accordingly.

4. Conclusion

This study found that UHMWPE particles are uneven and clump together, while PP particles are smoother and more uniform. This means that in a composite, PP will be the main material, and UHMWPE will help improve its flow. X-ray tests showed that PP is more crystalline (71.43 ± 0.50) than UHMWPE (63.63 ± 0.50). This difference affects how the two materials mix. The results suggest that the PP-UHMWPE composite is good for making bone implants using Fused Filament Fabrication (FFF) technology. In real-world use, this composite could improve bone implants by combining the best features of both materials. Future research should look at how the composite performs for bone replacement, including its strength and safety. It would also be useful to test how different printing settings affect the composite in FFF.

Acknowledgement

This research was supported by Ministry of Higher Education (MOHE) through Fundamental Research Grant Scheme (FRGS) FRGS/1/2023/TK09/UTHM/03/1 and Universiti Tun Hussein Onn Malaysia (UTHM) through GPPS (vot Q568).

Conflict of Interest

Authors declare that there is no conflict of interests regarding the publication of the paper.

Author Contribution

The authors confirm contribution to the paper as follows: ***Experimental work, Capture Data, First Author:*** *Fakrul Nur Aiman Raman;* ***Corresponding Author****: Kamarudin, K.;* ***Manuscript Preparation, Manuscript Improvement:*** *Fakrul Nur Aiman Raman, Kamarudin, K., Rahim Jamian, A. Ahmad;* ***Mixing Process Design:*** *Shufeng Sun;* ***Crushing Process:*** *M.F. Shaari;* ***Post Mixing, Characterization Work:*** *Mohd Nazrul Roslan, Mohd Khairuddin M.S, Raman.I. All authors reviewed the results and approved the final version of the manuscript.*

References

[1] S. V. Panin *et al.*, "Two-component feedstock based on ultra-high molecular weight polyethylene for additive manufacturing of medical products," *Advanced Industrial and Engineering Polymer Research*, vol. 4, no. 4, pp. 235–250, Oct. 2021, doi: 10.1016/j.aiepr.2021.05.003.

[2] S. C. Chowdhury, S. Sockalingam, and J. W. Gillespie Jr., "Inter-molecular interactions in ultrahigh molecular weight polyethylene single crystals," *Comput Mater Sci*, vol. 172, p. 109360, Feb. 2020, doi: 10.1016/j.commatsci.2019.109360.

[3] M. Abdul Samad, "Recent Advances in UHMWPE/UHMWPE Nanocomposite/UHMWPE Hybrid Nanocomposite Polymer Coatings for Tribological Applications: A Comprehensive Review," *Polymers (Basel)*, vol. 13, no. 4, p. 608, Feb. 2021, doi: 10.3390/polym13040608.

[4] M. Machado Rodrigues *et al.*, "Overview of sterilization methods for UHMWPE through surface analysis," *Mater Adv*, vol. 1, no. 9, pp. 3243–3255, 2020, doi: 10.1039/D0MA00772B.

[5] L. Han, H. Cai, X. Chen, C. Zheng, and W. Guo, "Study of UHMWPE Fiber Surface Modification and the Properties of UHMWPE/Epoxy Composite," *Polymers (Basel)*, vol. 12, no. 3, p. 521, Mar. 2020, doi: 10.3390/polym12030521.

[6] N. A. Patil, J. Njuguna, and B. Kandasubramanian, "UHMWPE for biomedical applications: Performance and functionalization," *Eur Polym J*, vol. 125, p. 109529, Feb. 2020, doi: 10.1016/j.eurpolymj.2020.109529.

[7] M. Xie, J. Chen, and H. Li, "Morphology and mechanical properties of injection-molded ultrahigh molecular weight polyethylene/polypropylene blends and comparison with compression molding," *J Appl Polym Sci*, vol. 111, no. 2, pp. 890–898, Jan. 2009, doi: 10.1002/app.29036.

[8] Y. Li, H. He, Y. Ma, Y. Geng, and J. Tan, "Rheological and mechanical properties of ultrahigh molecular weight polyethylene/high density polyethylene/polyethylene glycol blends," *Advanced Industrial and Engineering Polymer Research*, vol. 2, no. 1, pp. 51–60, Jan. 2019, doi: 10.1016/j.aiepr.2018.08.004.

[9] S. Spiegelberg, A. Kozak, and G. Braithwaite, "Characterization of Physical, Chemical, and Mechanical Properties of UHMWPE," in *UHMWPE Biomaterials Handbook*, Elsevier, 2016, pp. 531–552. doi: 10.1016/B978-0-323-35401-1.00029-6.

[10] E. M. Lee, H. M. Jeong, and B. K. Kim, "Mechanical, Thermal, and Surface Properties of Ultrahigh Molecular Weight Polyethylene/Polypropylene Blends," *Journal of Macromolecular Science, Part B*, vol. 49, no. 5, pp. 854–863, Aug. 2010, doi: 10.1080/00222341003600723.

[11] N. Vidakis *et al.*, "Fused Filament Fabrication 3D printed polypropylene/ alumina nanocomposites: Effect of filler loading on the mechanical reinforcement," *Polym Test*, vol. 109, p. 107545, May 2022, doi: 10.1016/j.polymertesting.2022.107545.

[12] S. Charlon, J. Le Boterff, and J. Soulestin, "Fused filament fabrication of polypropylene: Influence of the bead temperature on adhesion and porosity," *Addit Manuf*, vol. 38, p. 101838, Feb. 2021, doi: 10.1016/j.addma.2021.101838.

[13] F. Casamento, E. Padovano, S. Pappalardo, A. Frache, and C. Badini, "Development of polypropylene-based composites through fused filament fabrication: The effect of carbon-based fillers," *Compos Part A Appl Sci Manuf*, vol. 164, p. 107308, Jan. 2023, doi: 10.1016/j.compositesa.2022.107308.

[14] J. H. Yun, Y. J. Jeon, and M. S. Kang, "Analysis of Elastic Properties of Polypropylene Composite Materials with Ultra-High Molecular Weight Polyethylene Spherical Reinforcement," *Materials*, vol. 15, no. 16, Aug. 2022, doi: 10.3390/ma15165602.

[15] Q. Gao *et al.*, "Fabrication of new conductive surface-metallized UHMWPE fabric with improved thermal resistance," *RSC Adv*, vol. 10, no. 26, pp. 15139–15147, 2020, doi: 10.1039/D0RA02228D.

[16] S. V. Panin, L. A. Kornienko, V. O. Aleksenko, L. R. Ivanova, S. V. Shil'ko, and Yu. M. Pleskachevsky, "Extrudable Uhmwpe-Based Composites: Prospects Of Application In Additive Technologies," *Nanoscience and Technology: An International Journal*, vol. 8, no. 2, pp. 85–94, 2017, doi: 10.1615/NanoSciTechnolIntJ.v8.i2.10.

[17] S. V. Panin, L. A. Kornienko, V. O. Alexenko, D. G. Buslovich, and Yu. V. Dontsov, "Extrudable polymer-polymer composites based on ultra-high molecular weight polyethylene," 2017, p. 020005. doi: 10.1063/1.5017317.

[18] W. Zhu, C. Yan, Y. Shi, S. Wen, J. Liu, and Y. Shi, "Investigation into mechanical and microstructural properties of polypropylene manufactured by selective laser sintering in comparison with injection molding counterparts," *Mater Des*, vol. 82, pp. 37–45, Oct. 2015, doi: 10.1016/j.matdes.2015.05.043.

[19] N. Singh and S. K. Sinha, "Tribological Studies of Epoxy Composites With UHMWPE and MoS2 Fillers Coated on Bearing Steel: Dry Interface and Grease Lubrication," *J Tribol*, vol. 142, no. 5, May 2020, doi: 10.1115/1.4046015.
[20] G. Liu, M. Xiang, and H. Li, "A study on sliding wear of ultrahigh molecular weight polyethylene/polypropylene blends," *Polym Eng Sci*, vol. 44, no. 1, pp. 197–208, Jan. 2004, doi: 10.1002/pen.20018.
[21] G. Prashar, H. Vasudev, and D. Bhuddhi, "Additive manufacturing: expanding 3D printing horizon in industry 4.0," *International Journal on Interactive Design and Manufacturing*, vol. 17, no. 5, pp. 2221–2235, Oct. 2023, doi: 10.1007/s12008-022-00956-4.
[22] Y. Bozkurt and E. Karayel, "3D printing technology; methods, biomedical applications, future opportunities and trends," *Journal of Materials Research and Technology*, vol. 14, pp. 1430–1450, Sep. 2021, doi: 10.1016/j.jmrt.2021.07.050.
[23] D.-H. Yun, J.-H. Yun, Y.-J. Jeon, and M.-S. Kang, "Analysis of Elastic Properties According to the Aspect Ratio of UHMWPE Fibers Added to PP/UHMWPE Composites," *Applied Sciences*, vol. 12, no. 22, p. 11429, Nov. 2022, doi: 10.3390/app122211429.
[24] H. Cheng *et al.*, "Enhancement of Electromagnetic Interference Shielding Performance and Wear Resistance of the UHMWPE/PP Blend by Constructing a Segregated Hybrid Conductive Carbon Black–Polymer Network," *ACS Omega*, vol. 6, no. 23, pp. 15078–15088, Jun. 2021, doi: 10.1021/acsomega.1c01240.
[25] O. V. Gogoleva, P. N. Petrova, E. S. Kolesova, and A. A. Okhlopkova, "Influence of Component–Mixing Methods on the Properties and Structure of UHMWPE-Based Composites," *Journal of Friction and Wear*, vol. 41, no. 1, pp. 36–39, Jan. 2020, doi: 10.3103/S1068366620010080.
[26] V. Gavande, M. Jeong, and W.-K. Lee, "On the Mechanical, Thermal, and Rheological Properties of Polyethylene/Ultra-High Molecular Weight Polypropylene Blends," *Polymers (Basel)*, vol. 15, no. 21, p. 4236, Oct. 2023, doi: 10.3390/polym15214236.
[27] D. Laurence, L. Aanen, and J. Westerweel, "Engineering Turbulence Modelling and Experiments-4 W Measurements on the mixing of a passive scalar in a turbulent pipe flow using DPIV and LIF."
[28] D.-H. Yun, J.-H. Yun, Y.-J. Jeon, and M.-S. Kang, "Analysis of Elastic Properties According to the Aspect Ratio of UHMWPE Fibers Added to PP/UHMWPE Composites," *Applied Sciences*, vol. 12, no. 22, p. 11429, Nov. 2022, doi: 10.3390/app122211429.
[29] L. Qi, L. Wu, R. He, H. Cheng, B. Liu, and X. He, "Synergistic toughening of polypropylene with ultra-high molecular weight polyethylene and elastomer-olefin block copolymers," *RSC Adv*, vol. 9, no. 41, pp. 23994–24002, 2019, doi: 10.1039/C9RA01073D.
[30] M. Jin, B. Jin, X. Xu, X. Li, T. Wang, and J. Zhang, "Effects of ultrahigh molecular weight polyethylene and mould temperature on morphological evolution of isotactic polypropylene at micro-injection moulding condition," *Polym Test*, vol. 46, pp. 41–49, Sep. 2015, doi: 10.1016/j.polymertesting.2015.06.018.
[31] D.-H. Yun, J.-H. Yun, Y.-J. Jeon, and M.-S. Kang, "Analysis of Elastic Properties According to the Aspect Ratio of UHMWPE Fibers Added to PP/UHMWPE Composites," *Applied Sciences*, vol. 12, no. 22, p. 11429, Nov. 2022, doi: 10.3390/app122211429.
[32] O. V. Gogoleva, P. N. Petrova, E. S. Kolesova, and A. A. Okhlopkova, "Influence of Component–Mixing Methods on the Properties and Structure of UHMWPE-Based Composites," *Journal of Friction and Wear*, vol. 41, no. 1, pp. 36–39, Jan. 2020, doi: 10.3103/S1068366620010080.
[33] V. Gavande, M. Jeong, and W.-K. Lee, "On the Mechanical, Thermal, and Rheological Properties of Polyethylene/Ultra-High Molecular Weight Polypropylene Blends," *Polymers (Basel)*, vol. 15, no. 21, p. 4236, Oct. 2023, doi: 10.3390/polym15214236.
[34] M. Hussain *et al.*, "Ultra-High-Molecular-Weight-Polyethylene (UHMWPE) as a Promising Polymer Material for Biomedical Applications: A Concise Review," *Polymers (Basel)*, vol. 12, no. 2, p. 323, Feb. 2020, doi: 10.3390/polym12020323.
[35] S. Kaboli *et al.*, "Behavior of Solid Electrolyte in Li-Polymer Battery with NMC Cathode via in-Situ Scanning Electron Microscopy," *Nano Lett*, vol. 20, no. 3, pp. 1607–1613, Mar. 2020, doi: 10.1021/acs.nanolett.9b04452.
[36] S. Nejatbakhsh *et al.*, "Improvement of the Bioactivity of UHMWPE by Two Different Atmospheric Plasma Treatments," *Plasma Chemistry and Plasma Processing*, vol. 41, no. 1, pp. 245–264, Jan. 2021, doi: 10.1007/s11090-020-10134-7.
[37] E. Enqvist and N. Emami, "Nanodiamond reinforced ultra high molecular weight polyethylene for orthopaedic applications: dry versus wet ball milling manufacturing methods," *Tribology - Materials, Surfaces & Interfaces*, vol. 8, no. 1, pp. 7–13, Mar. 2014, doi: 10.1179/1751584X13Y.0000000059.
[38] T. H. Lee, F. Y. C. Boey, and K. A. Khor, "X-ray diffraction analysis technique for determining the polymer crystallinity in a polyphenylene sulfide composite," *Polym Compos*, vol. 16, no. 6, pp. 481–488, Dec. 1995, doi: 10.1002/pc.750160606.

[39] Y. Tkachenko and P. Niedzielski, "FTIR as a Method for Qualitative Assessment of Solid Samples in Geochemical Research: A Review," *Molecules*, vol. 27, no. 24, p. 8846, Dec. 2022, doi: 10.3390/molecules27248846.
[40] M. M. Eid, "Characterization of Nanoparticles by FTIR and FTIR-Microscopy," in *Handbook of Consumer Nanoproducts*, Singapore: Springer Singapore, 2021, pp. 1–30. doi: 10.1007/978-981-15-6453-6_89-1.
[41] S. Magalhães, B. J. Goodfellow, and A. Nunes, "FTIR spectroscopy in biomedical research: how to get the most out of its potential," *Appl Spectrosc Rev*, vol. 56, no. 8–10, pp. 869–907, Nov. 2021, doi: 10.1080/05704928.2021.1946822.
[42] M. C. Galetz and U. Glatzel, "Molecular Deformation Mechanisms in UHMWPE During Tribological Loading in Artificial Joints," *Tribol Lett*, vol. 38, no. 1, pp. 1–13, Apr. 2010, doi: 10.1007/s11249-009-9563-y.
[43] V. Saikko, "Adverse condition testing with hip simulators," *Biotribology*, vol. 1–2, pp. 2–10, Mar. 2015, doi: 10.1016/j.biotri.2015.02.001.
[44] V. Saikko and M. Shen, "Wear comparison between a dual mobility total hip prosthesis and a typical modular design using a hip joint simulator," *Wear*, vol. 268, no. 3–4, pp. 617–621, Feb. 2010, doi: 10.1016/j.wear.2009.10.011.
[45] J. Domínguez-Robles *et al.*, "Lignin/poly(butylene succinate) composites with antioxidant and antibacterial properties for potential biomedical applications," *Int J Biol Macromol*, vol. 145, pp. 92–99, Feb. 2020, doi: 10.1016/j.ijbiomac.2019.12.146.
[46] M. Fareed Hafizuddin Md Fadil and M. Yussni Hashim, "Mechanical Properties of Recycle Polymers Reinforcement with Glass Fiber Composite Material," *Research Progress in Mechanical and Manufacturing Engineering*, vol. 2, no. 2, pp. 227–234, 2021, doi: 10.30880/rpmme.2021.02.02.027.
[47] M. T. H. Siddiqui *et al.*, "Thermal, mechanical, rheological, electrical and electromagnetic interference shielding performance of polypropylene/magnetic carbon nanocomposites," *J Environ Chem Eng*, vol. 9, no. 4, p. 105447, Aug. 2021, doi: 10.1016/j.jece.2021.105447.
[48] M. Yuan, G. Zhang, B. Li, T. C. M. Chung, R. Rajagopalan, and M. T. Lanagan, "Thermally Stable Low-Loss Polymer Dielectrics Enabled by Attaching Cross-Linkable Antioxidant to Polypropylene," *ACS Appl Mater Interfaces*, vol. 12, no. 12, pp. 14154–14164, Mar. 2020, doi: 10.1021/acsami.0c00453.
[49] H. R. Nafchi, M. Abdouss, S. K. Najafi, R. M. Gargari, and M. Mazhar, "Effects of nano-clay particles and oxidized polypropylene polymers on improvement of the thermal properties of wood plastic composite," *Maderas. Ciencia y tecnología*, no. ahead, pp. 0–0, 2015, doi: 10.4067/S0718-221X2015005000005.
[50] P. Dong *et al.*, "Pursuit of the correlation between yield strength and crystallinity in sintering-molded UHMWPE," *Polymer (Guildf)*, vol. 215, p. 123352, Feb. 2021, doi: 10.1016/j.polymer.2020.123352.